Dynamics of a semiconductor laser array with delayed global coupling

G. Kozyreff,[1] A. G. Vladimirov,[2] and Paul Mandel[1]
[1]*Optique Nonlinéaire Théorique, Université Libre de Bruxelles, Campus Plaine CP 231, B-1050 Bruxelles, Belgium*
[2]*Physics Faculty, St. Petersburg State University, 198904 St. Petersburg, Russia*
(Received 10 January 2001; published 26 June 2001)

We study the dynamics of an array of single mode semiconductor lasers globally but weakly coupled by a common external feedback mirror and by nearest neighbor interactions. We seek to determine the conditions under which all lasers of the array are in phase, whether in a steady, periodic, quasiperiodic, or chaotic regime, in order to maximize the output far field intensity. We show that the delay may be a useful control parameter to achieve in-phase synchronization. For the in-phase steady state, there is a competition between a delay-induced Hopf bifurcation leading to an in-phase periodic regime and a delay-independent Hopf bifurcation leading to an antiphased periodic regime. Both regimes are described analytically and secondary Hopf bifurcations to quasiperiodic solutions are found. Close to the stable steady state, the array is described by a set of Kuramoto equations for the phases of the fields. Above the first Hopf bifurcation, these equations are generalized by the addition of second and third order time derivatives of the phases.

DOI: 10.1103/PhysRevE.64.016613 PACS number(s): 42.55.−f, 42.60.Da

I. INTRODUCTION

Many physical, chemical, and biological systems consist of interacting elementary units. A general class of such systems is that of weakly coupled oscillators. If the coupling does not modify significantly the phase space trajectories, one phase variable suffices to describe each oscillating element. This leads to phase models, including the extensively studied Kuramoto equations [1,2]. In recent years, it was realized that delaying the interactions between elementary cells can have a profound influence on their collective behavior. The principal consequences of time delay documented for phase models concern the occurrence of synchronization [3,4] and multistability between states of synchronization [5]. However, if the coupling strength is comparable to the attraction to the limit cycle, amplitude quenching or ''oscillation death'' can also result from the delay [6]. From the general viewpoint of coupled oscillators, the physical system we study in the present paper mixes the two situations. We consider an array of semiconductor lasers (SCL's) that are weakly and globally coupled by the optical feedback of an external mirror. For very small values of the coupling strength, the electric fields emitted by each SCL are essentially described by their optical phases, and the system can be modeled by phase equations of the Kuramoto type. However, increasing the coupling strength gives rise to time periodic intensities by way of a Hopf bifurcation. The amplitude of the limit cycle created by this mechanism strongly depends on the coupling strength. Each element of the array thus becomes a two-frequency oscillator with one frequency in the optical domain and the other frequency corresponding to sustained relaxation oscillations and typically lying in the GHz range for a SCL. To investigate the dynamics of this system, we have suggested an extension of the Kuramoto model [7].

Aside from its fundamental interest, this subject has a technological application. SCL arrays are a compact and high power optical source. To concentrate the maximum coherent output power in a single lobed far field pattern, it is required to lock the SCL elements in phase. For this, the symmetry of the coupling is an essential characteristic of the system. It was indeed found theoretically [8], in the absence of delay, that a global coupling is more suitable than a nearest-neighbor coupling to synchronize the SCL's in phase. Numerical simulations tend to extend this conclusion to the case where the coupling is delayed [9]. On the other hand, phase locking was investigated in a laser array with a random distribution of frequencies and instantaneous global coupling [10]. The idea to use optical feedback in order to synchronize a laser array was already exploited in Ref. [11]. However, up to now, only strong coupling has been considered, which raises some technical difficulties. The very small transverse size of the SCL's makes it difficult to efficiently reinject a substantial fraction of the emitted field back into their active region. Usually, the mirror is placed a few millimeters away from the array, for instance at the Talbot distance. With such a small external cavity length, the only effect of the delay is to change the phase of the reinjected field.

In this paper, we again consider the model discussed in Ref. [7]: a one-dimensional array of SCL's with possibly nearest-neighbor coupling, with a global coupling of the lasers by a spherical mirror placed centimeters away from the array, as depicted in Fig. 1. The spherical shape of the mirror minimizes the optical path difference between SCL's. Such a spherical feedback mirror was recently used to stabilize the emission of a broad area laser [12]. Since we consider only a weak coupling between the lasers in our model, the feedback field is assumed to be smaller by orders of magnitude than in Ref. [11]. We give a detailed and extended analysis of the model presented in Ref. [7]. Our purpose is to determine how to maximize the array output. This goal is achieved if the lasers are phase locked, which in this case means that they should be in phase. We show that the problem is phase sensitive, and that the cw regimes can be either in-phase or out of phase. The in-phase steady state can bifurcate toward a time periodic regime, following two different routes, and the array can be either in phase or antiphase in this time

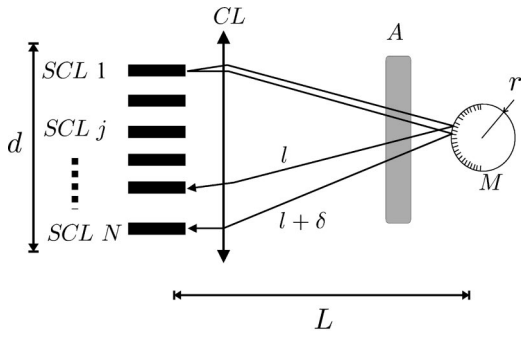

FIG. 1. Schematic representation of a SCL array with global optical coupling between the lasers. d is the transverse size of the array. The spherical feedback mirror M of radius r is placed at the focus of the converging lens CL, and at a distance L from the array. A is an attenuator, controlling the strength of the coupling.

periodic regime. The bifurcation to the in-phase time periodic regime does not exist in the absence of a delayed feedback. It is therefore a delay-induced bifurcation. Maximization of the array output is achieved if parameters are selected such that the bifurcation occurs toward the in-phase periodic regime.

This paper is organized as follows. In Sec. II, we describe the model and introduce the evolution equations. In Secs. III and IV, we study the synchronization properties of the SCL array in the cw regime. We calculate the self-pulsing thresholds from the cw states. For the in-phase steady state, there are two possible thresholds: a degenerate Hopf bifurcation leading to antiphase periodic laser intensities, and a regular Hopf bifurcation leading to in-phase periodic laser intensities. In Sec. V, we present an analytical treatment of the synchronization in the self-pulsing domain in the simplifying limit of a large linewidth enhancement factor α. This results from an explicit derivation of evolution equations governing the slow time dependence of the laser intensities, also known as the solvability condition of the bifurcation equations.

II. MODEL

The mathematical model of our system is a set of N coupled Lang-Kobayashi equations in dimensionless form

$$\frac{dE_j}{dt} = i\omega_j E_j + (1+i\alpha)Z_j E_j + i\frac{\chi}{2}e^{-i\zeta}(E_{j-1}+E_{j+1}) + i\frac{\eta}{N}\sum_{n=1}^{N} e^{-i(\vartheta_{jn}+\bar{\vartheta})}E_n(t-t_D), \quad (1)$$

$$\gamma^{-1}\frac{dZ_j}{dt} = P_j - Z_j - (1+2Z_j)|E_j|^2, \quad (2)$$

with periodic boundary conditions $E_0=E_N$, $E_{N+1}=E_1$. In Eqs. (1) and(2), E_j is the electric field, and Z_j is the carrier excess density of the jth laser. The time unit is the photon cavity lifetime $\tau_p \simeq 2\times 10^{-12}$ s. $\gamma=\tau_p/\tau_c \simeq 10^{-3}$ is the ratio of the photon to carrier lifetimes, and $\alpha \simeq 5$ is the linewidth enhancement factor. P_j is the excess pump parameter of laser j, which is proportional to the injection current above threshold. We suppose that all lasers operate in the same single longitudinal mode of the short cavity. This may require the use of frequency
slection techniques [13], or require one to pump the lasers not too far above the lasing threshold. The jth laser has a lasing frequency ω_j/τ_p in the absence of optical feedback and coupling between the lasers. We denote by $\bar{P}$ and $\bar{\omega}$ the average pump and optical frequency over the SCL array. Hereafter we will assume that the deviations $|P_j-\bar{P}|$ and $|\omega_j-\bar{\omega}|$ are small.

The parameter η describes the global coupling strength. The phase of the fields reinjected in the array of SCL's is $\vartheta_{nj}+\bar{\vartheta}$, and $t_D=2L/(c\tau_p)$ is the external cavity round-trip time normalized by τ_p. Note that, for symmetry reasons, in Eqs. (1) and(2) we do not follow the commonly adopted notations in which the feedback term appears without an imaginary unit i [14]. This, however, is equivalent to setting $\bar{\vartheta}=\pi/2$, or shifting the position of the external mirror by one eighth of the optical wavelength. Since the exact value of the external cavity length is not known with precision, we may simply set $\bar{\vartheta}$ equal to zero. The phase dispersion $|\vartheta_{nj}| \equiv \bar{\omega}|\delta_{nj}|/c$ can be made small if the feedback mirror (with radius $r \ll L$) is placed at the focus of a converging lens and sufficiently far from the SCL array (see Fig. 1). Indeed, if the lateral dimension d of the array is small compared to the external cavity length L, one has an inequality $|\delta_{nj}| \lesssim r(d/2L)^2$. For instance, if $d=1$ mm, $r=1$ mm, and $L=10$ cm, the dispersion in the optical path lengths is $|\delta_{nj}| \lesssim 2.5\times 10^{-8}$ m, which is much shorter than one optical wavelength. Hereafter, theoretical conclusions will therefore be stated for $\vartheta_{nj}=0$. The parameters χ and ζ measure, respectively, the strength and the phase of the local coupling that can arise due to the interaction between neighboring lasers via evanescent fields. Note that the phase of the local coupling ζ is usually assumed to be zero [15]. Finally, we will assume that the coupling between the lasers is weak: $\eta,\chi \ll 1$.

III. SYNCHRONIZATION BELOW SELF-PULSING THRESHOLD

A. In-phase synchronization

In this section, we derive the steady states of Eqs. (1) and (2). These equations are phase sensitive, and admit in-phase and antiphase solutions. In this problem, steady states are defined by the property that the laser intensities are constant. We study the linear stability of the in-phase and antiphase cw regimes. Since we are mainly interested in the effect of time delay on the synchronization of globally coupled lasers, we present a detailed stability analysis for the case $\chi=0$, and only briefly discuss the influence of the local coupling on the stability properties of cw states. The optical feedback can destabilize the SCL array from its cw operation. However, before η exceeds the self-pulsing threshold, the SCL's deliver a constant intensity. Below this threshold, the stability of the steady state justifies that Z_j and the modulus of the fields $|E_j|$ can be adiabatically eliminated in Eqs. (1) and (2).

In the limit $|P_j/\bar{P}-1|=|\delta P_j|\ll 1$, this yields the following set of coupled equations for the field phases:

$$\frac{d\phi_j}{dt}=\omega_j-\frac{\eta}{N}\sqrt{1+\alpha^2}\times\sum_{n=1}^{N}\sin[\vartheta_{jn}+\phi_j-\phi_n(t-t_D)-\cot^{-1}\alpha]-\frac{\chi}{2}\sqrt{1+\alpha^2}\sum_{q=1,-1}\sin(\phi_j-\phi_{j+q}+\zeta-\cot^{-1}\alpha), \tag{3}$$

with the boundary conditions $\phi_0=\phi_N$ and $\phi_{N+1}=\phi_1$. Note that the effective coupling strength in Eq. (3) is proportional to $\sqrt{1+\alpha^2}$, and therefore increases with the linewidth enhancement factor α. If local interactions are negligible, $\chi\ll\eta$, and if $|\vartheta_{jn}|\ll 1$, Eq. (3) reduces to the Kuramoto equations with a time delay [3,4].

Let all the lasers be identical, so that $\omega_j=\bar{\omega}$. The in-phase solutions of Eq. (3) are given by $\phi_j=\omega t$, with the common frequency ω obeying the transcendental equation

$$\omega=\bar{\omega}-\sqrt{1+\alpha^2}[\eta\sin(\omega t_D-\cot^{-1}\alpha)+\chi\sin(\zeta-\cot^{-1}\alpha)]. \tag{4}$$

This equation can have multiple solutions. They correspond to the external cavity modes (ECM's) of the single laser [14], which grow in number with increasing ηt_D. The linear stability analysis of the in-phase cw state can be performed by substituting

$$\phi_j=\omega t+\varepsilon\sum_{k=1}^{N}\delta\phi_k e^{2ijk/N} \tag{5}$$

into Eq. (3) and collecting $O(\varepsilon)$ terms. The linearized equations for $\delta\phi_k$ yield the stability conditions

$$\eta\cos(\omega t_D-\cot^{-1}\alpha)+2\chi\cos(\zeta-\cot^{-1}\alpha)\sin^2\left(\frac{k\pi}{N}\right)>0, \tag{6}$$

where $k=1,\ldots,N-1$. The effect of the local coupling on the stability of the in-phase cw regimes depends on the relative phase between the global and local couplings. If the two cosine functions in Eq. (6) have the same sign for large N, local coupling almost does not change the stability domain of the cw in-phase solution. Otherwise this stability domain decreases with increasing local coupling strength χ. This was also observed in Ref. [16].

Letting $\chi\to 0$, the bifurcations defined by Eq. (6) merge into a single $(N-1)$-fold degenerate bifurcation. Then, successively solving Eqs. (6) and (4), one finds instability domains of the in-phase cw state which are triangles in the $(\bar{\omega}t_D,\eta)$ parameter plane,

$$\frac{\pi}{2}+\eta t_D\sqrt{1+\alpha^2}\leqslant\bar{\omega}t_D-\cot^{-1}(\alpha)-2n\pi\leqslant\frac{3\pi}{2}-\eta t_D\sqrt{1+\alpha^2}, \tag{7}$$

where n is an arbitrary integer. These inequalities are consistent with results derived in Ref. [3], and obtained in the limit $N\to\infty$. In Eq. (7) the time delay appears on two well separated time scales: $\bar{\omega}t_D$ and ηt_D. Since $\eta\ll 1\ll\bar{\omega}$, the variation of the external cavity length L over one optical wavelength leads to a variation of 4π for $\bar{\omega}t_D$, but leaves ηt_D almost constant. Therefore, we can consider $\bar{\omega}t_D$, and ηt_D as independent parameters of the problem. Inside the domain defined by Eq. (7), in-phase synchronization is lost in favor of antiphase cw regimes. The size of these instability domains is inversely proportional to ηt_D. Therefore, to increase the time delay favors in-phase cw operation. In Sec. IV, we shall define selfpulsing thresholds η_{H1} and η_{H2} to periodic intensities. If t_D is sufficiently large and if $\pi(2t_D\sqrt{1+\alpha^2})^{-1}<\eta<\eta_{H1,2}$, stable cw in-phase operation exists for all values of $\bar{\omega}t_D$. This is due to the overlap of stability domains of cw in-phase solutions corresponding to different ECM's.

B. Antiphase synchronization

The antiphase cw solutions are defined by

$$\phi_j=\bar{\omega}t+2jM\pi/N, \tag{8}$$

where the integer M determines the type of antiphase state. The stability conditions for Eq. (8) can be obtained using a discrete Fourier transformation similar to Eq. (5). They are

$$\chi\cos(\zeta-\cot^{-1}\alpha)\cos\left(\frac{2M\pi}{N}\right)\sin^2\left(\frac{k\pi}{N}\right)>0, \tag{9}$$

with $k=1,\ldots,N$, $k\neq M,N-M$ and

$$\eta\cos(\omega t_D-\cot^{-1}\alpha)-4\chi\cos(\zeta-\cot^{-1}\alpha)\cos\left(\frac{2M\pi}{N}\right)\sin^2\left(\frac{M\pi}{N}\right)<0, \tag{10}$$

where ω verifies the transcendental equation:

$$\omega=\bar{\omega}-\sqrt{1+\alpha^2}\left[\frac{\eta}{2}\sin(\omega t_D-\cot^{-1}\alpha)+2\chi\sin^2\left(\frac{M\pi}{N}\right)\sin(\zeta-\cot^{-1}\alpha)\right]. \tag{11}$$

The stability boundaries defined by Eqs. (9) and (10) correspond to Hopf bifurcations with the frequency $\omega-\bar{\omega}$. According to the stability condition [Eq. (9)], the local coupling selects the antiphase states with M such that $\cos(\zeta-\cot^{-1}\alpha)\cos(2M\pi/N)>0$. It then follows from Eq. (10) that the stability domain of these states increases with χ.

In the absence of local coupling, the left hand side of Eq. (9) vanishes, which implies that the antiphase state [Eq. (8)] is neutrally stable with $N-2$ zero eigenvalues. In addition, there is a zero eigenvalue associated with the invariance under the global phase shift $\phi_j \to \phi_j + \text{const}$. This neutral stability is related to the existence of a $(N-1)$-dimensional invariant manifold in the phase space of Eq. (3). It is the manifold spanned by the antiphase solutions that verify the relation $\Sigma_j \exp(i\phi_j)=0$ [16–18]. Expressions (10) and (11) yield the following neutral stability domains of the antiphase cw solutions [Eq. (8)]:

$$\frac{\pi}{2} + \frac{\eta t_D}{2}\sqrt{1+\alpha^2} \leqslant \bar{\omega} t_D - \cot^{-1}\alpha - 2n\pi \leqslant \frac{3\pi}{2} - \frac{\eta t_D}{2}\sqrt{1+\alpha^2}. \tag{12}$$

Finally, we note that the phase equations (3) are valid in the limit $\eta, \chi, |\delta P_j| \ll 1$, and below the self-pulsing threshold. Under these assumptions, the stability conditions obtained in this section agree with the linear stability analysis of the full equations (1) and (2).

Let us now relax the assumption $\omega_j = \bar{\omega}$. Then, in the large N limit, assuming a Lorentzian distribution for the natural frequencies, $g(\omega') = (\Gamma/\pi)[\Gamma^2 + (\omega' - \bar{\omega})^2]^{-1}$, the stability condition for the desynchronized state becomes [3,4]

$$\eta < \eta_c \equiv \frac{2\Gamma}{\sqrt{1+\alpha^2}\cos(\omega t_D - \cot^{-1}\alpha)}, \tag{13}$$

where ω verifies Eq. (11) with $\eta = \eta_c$ and $\chi = 0$. Note that, as $\Gamma \to 0$, the stability boundary defined by Eq. (13) transforms into Eq. (10), with $\chi = 0$.

IV. SELF-PULSING INSTABILITIES

A. Antiphase Hopf bifurcation

In order to describe Hopf bifurcations of the in-phase cw state leading to solutions with self-pulsing laser intensities, we return to the original set of coupled Lang-Kobayashi equations (1) and (2). We confine our treatment to the case of identical lasers by setting $\omega_j = \bar{\omega}$ and $P_j = \bar{P}$. The complete in-phase cw solution of Eqs. (1) and (2) is then

$$E_j(t) = \left(\frac{\bar{P} + \eta\sin(\omega t_D) + \chi\sin\zeta}{1 - 2\eta\sin(\omega t_D) - 2\chi\sin\zeta}\right)^{1/2} e^{i\omega t}, \tag{14}$$

$$Z_j(t) = -\eta\sin(\omega t_D) - \chi\sin\zeta, \tag{15}$$

where ω is the solution of Eq. (4). Besides the desynchronization boundaries [Eqs. (7)], a linear stability analysis of Eqs. (14) and (15) reveals the existence of two different types of Hopf bifurcations, leading to self-pulsing solutions. The bifurcations of the first type are associated with perturbations transverse to the synchronization manifold $\{E_1 = \cdots = E_N, Z_1 = \cdots = Z_N\}$. In the limit $\eta, \chi, \gamma \ll 1$, these bifurcations are defined by the condition

$$\eta = \eta_{H1}(k) \equiv \sec(\omega t_D + \cot^{-1}\alpha) \times \left[\frac{\gamma(1+2\bar{P})}{\sqrt{1+\alpha^2}} - 2\chi\sin^2\left(\frac{\pi k}{N}\right)\cos(\zeta + \cot^{-1}\alpha)\right], \tag{16}$$

with $k = 1, \ldots, N-1$. The associated relaxation oscillation frequency is $(2\gamma\bar{P})^{1/2}$. If $\cos(\zeta + \cot^{-1}\alpha) < 0$, the lowest bifurcation threshold [Eq. (16)] corresponds to $k=1$. In the limit $N \to \infty$, it coincides with the threshold in the absence of local coupling. Conversely, if $\cos(\zeta + \cot^{-1}\alpha) > 0$, the self-pulsing threshold is lowered by the local coupling, even for large N.

For $\chi = 0$, Eq. (16) gives a single boundary $\eta = \eta_{H1}$ associated with an $(N-1)$-fold degenerate Hopf bifurcation. Such a degenerate bifurcation is known to produce multiple branches of antiphase self-pulsing solutions [19]. The antiphase character of the emerging sustained relaxation oscillations partially destroys the in-phase synchronization of the cw state. The solutions describing these oscillations will be constructed in Sec. IV B.

B. In-phase Hopf bifurcation

Another Hopf bifurcation, which is always nondegenerate, is located at

$$\eta = \eta_{H2} \equiv \frac{\eta_{H1}}{1-\cos\varphi}, \quad \varphi \equiv \Omega_{H2} t_D. \tag{17}$$

Note that the bifurcation condition [Eq. (17)] is independent of χ, and is identical to that of a solitary laser with a feedback strength η instead of η/N in Eq. (1). The frequency Ω_{H2} characterizing the oscillations at $\eta = \eta_{H2}$ satisfies the transcendental equation

$$\Omega_{H2} = (2\gamma\bar{P})^{1/2} + \gamma(\bar{P} + 1/2)\cot\left(\frac{\Omega_{H2} t_D}{2}\right). \tag{18}$$

This equation has an infinity of solutions, each producing a different η_{H2} through the value of φ in Eq. (17). The periodic solution that bifurcates at $\eta = \eta_{H2}$ lies within the synchronization manifold. It is therefore characterized by in-phase synchronization, not only in the optical frequency ω but also in the relaxation oscillations at frequency Ω_{H2}.

Which of the two Hopf bifurcations, $\eta = \eta_{H1}$ or $\eta = \eta_{H2}$, takes place first and, hence, destabilizes the cw solution depends on the order of magnitude of the time delay t_D? We discuss three different situations: (i) small, (ii) moderate, and (iii) large delays.

(i) If $t_D \ll \gamma^{-1/2}$, then $\varphi \ll 1$ and the cw solutions (14) and (15) can only be destabilized through the Hopf bifurcation at

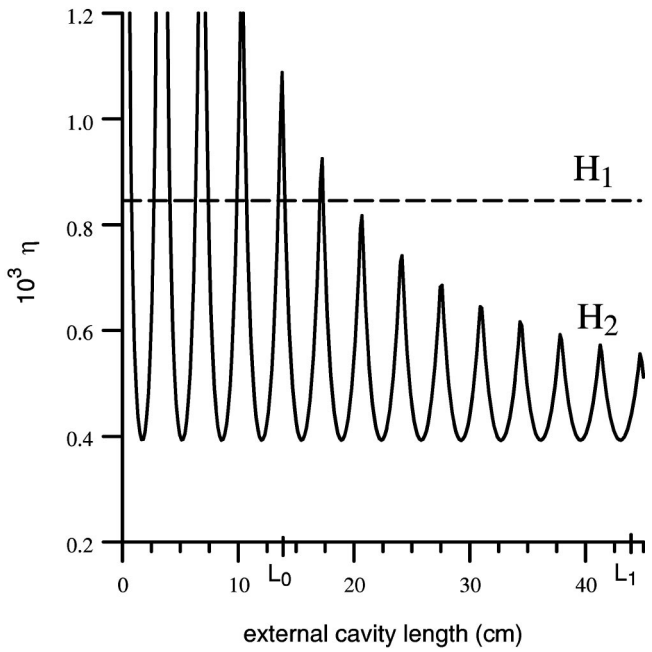

FIG. 2. Relative positions of the two Hopf bifurcations. $\chi=0$, $\alpha=5$, $P=1.5$, and $\gamma=10^{-3}$. The dashed line H_1 shows the minimal coupling strength necessary to reach the degenerate Hopf bifurcation $\eta=\eta_{H1}$. It corresponds to the minima of the curves H_1 shown in Fig. 3. The solid line H_2 represents the minimal coupling strength corresponding to the in-phase Hopf bifurcation $\eta=\eta_{H2}$, calculated using Eq. (17).

$\eta=\eta_{H1}$. In this limit, however, the phase dispersions ϑ_{nj} may become non negligible, which makes the validity of formula (16) questionable.

(ii) If $t_D\sim\gamma^{-1/2}$, i.e., the time delay is comparable to the relaxation oscillations period. The value of φ corresponding to the lowest bifurcation threshold η_{H2} is well approximated by $(2\gamma\overline{P})^{1/2}t_D$. Then the relative position of η_{H1} and η_{H2} can be controlled through φ by changing the external cavity length on the centimeter scale.

(iii) Finally, if $t_D\gtrsim\pi\gamma^{-1}(2\overline{P}+1)^{-1}$ there exists at least one solution Ω_{H2} of Eq. (18) such that $\eta_{H2}<\eta_{H1}$. Therefore, it is always the in-phase Hopf bifurcation [Eq. (17)] that destabilizes the in-phase cw solution. Moreover, our numerical simulations indicate that for large delays the in-phase synchronized self-pulsing solution emerging at $\eta=\eta_{H2}$ is stable in a wide domain above the desynchronization threshold given by $\eta=\eta_{H1}$. In this sense, the antiphase instability is bypassed, and in-phase synchronization is preserved by the in-phase Hopf bifurcation at $\eta=\eta_{H2}$.

Figure 2 illustrates the dependence of the minimal coupling strength necessary for the Hopf bifurcations $\eta=\eta_{H1}$ and $\eta=\eta_{H2}$ on the time delay. From Eqs. (16) and (17), η_{H1} and η_{H2} have minima $\eta_{H1}=\gamma(1+2\overline{P})/\sqrt{1+\alpha^2}$ and $\eta_{H2}=\eta_{H1}/(1-\cos\varphi)$ at $\cos(\omega t_D+\cot^{-1}\alpha)=1$. These minima are shown as functions of the external cavity length L. One can see that for $L\lesssim 20$ cm the order of appearance of the two Hopf bifurcations, $\eta=\eta_{H1}$ and $\eta=\eta_{H2}$, can be controlled through L. For larger L, the in-phase Hopf bifurcation always precedes the antiphase Hopf bifurcation.

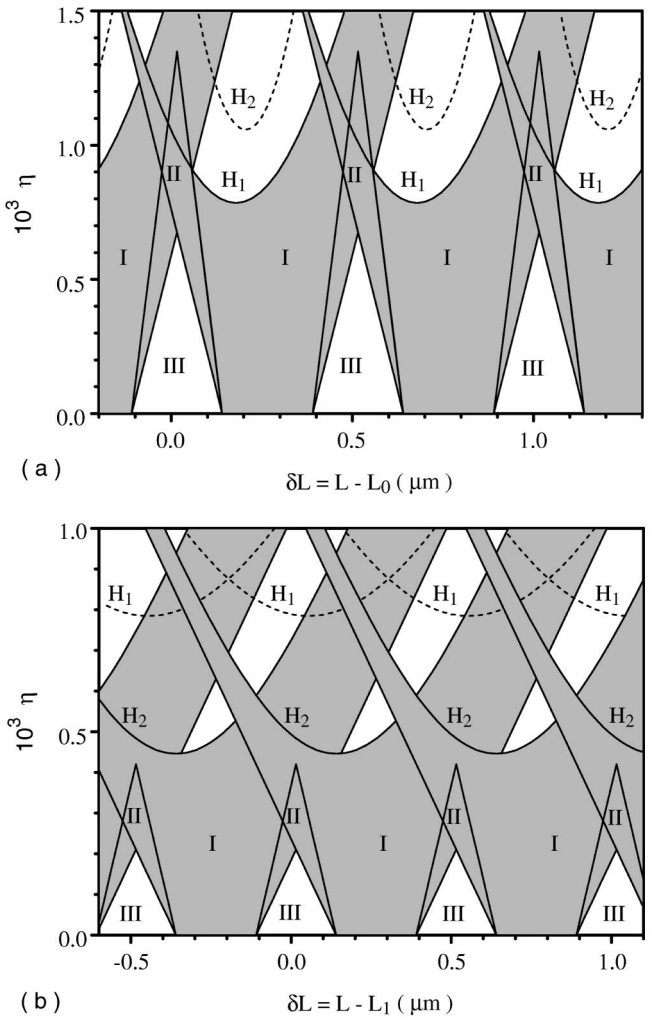

FIG. 3. Stability boundaries of cw solutions. The parameters are the same as in Fig. 2. (a) $L=L_0+\delta L$ and (b) $L=L_1+\delta L$ with $L_0=13.7$ cm and $L_1=44$ cm. In-phase states corresponding to different ECM's are stable in the grey areas (I and II). In the regions II stable antiphase and in-phase states coexist. In the white triangular regions III, only antiphase states are stable. Curves $H_{1,2}$ indicate the locations of Hopf bifurcations.

The linear stability analysis of the cw states is summarized in Figs. 3(a) and 3(b) for values of the external cavity length in the vicinity of $L\simeq 13.7$ and 44 cm, respectively. In these figures, L varies on the scale of the optical wavelength, which we fix at $\lambda=1$ μm. The gray areas labeled I and II are the stability domains of different cw in-phase solutions, each corresponding to a certain ECM. In Fig. 3(a), it is the Hopf bifurcation to antiphase self-pulsing solutions at $\eta=\eta_{H1}<\eta_{H2}$, which takes place first and destabilizes the in-phase cw state. In Fig. 3(b), corresponding to a larger value of feedback delay, the first Hopf bifurcation leading to in-phase self-pulsing regime takes place at $\eta=\eta_{H2}<\eta_{H1}$.

Having determined the critical coupling strengths η_{H1} and η_{H2}, we can complete the conditions to achieve synchronization in the cw operation,

$$\eta_c<\eta<\eta_{H1},\eta_{H2},$$

where η_c is defined in Eq. (13). Qualitatively, this imposes that the dispersion of the natural frequencies Γ be smaller than the relaxation rate of the carrier density γ.

Finally we conclude that according to the linear stability analysis, a large time delay favors in-phase synchronization, because it reduces the size of the instability domains [Eq. (7)] of the cw in-phase state, and favors the in-phase Hopf bifurcation at $\eta=\eta_{H2}$ against the antiphase bifurcation at $\eta=\eta_{H1}$.

V. SELF-PULSING SOLUTIONS

We now construct the time periodic solutions that bifurcate from the in-phase cw solutions (14) and (15). For the sake of mathematical convenience, we assume that $\alpha \gg 1$. Using this approximation, it is possible to describe analytically not only small amplitude self-pulsing solutions of Eqs. (1) and (2) near Hopf bifurcation thresholds, but finite amplitude periodic intensity solutions as well. Although, in practice, $\alpha \simeq 5$, the agreement with numerical results is quite remarkable. Working in the limit $\gamma,\eta,\chi,\alpha^{-1} \ll 1$, we seek a solution of Eqs. (1) and (2) of the following forms:

$$E_j(t)=\sqrt{P_j}\left(1+\frac{y_j}{\alpha}\right)\exp(i\Phi_j), \tag{19}$$

$$Z_j(t)=\Omega_j\frac{x_j}{\alpha}, \quad \Omega_j=\sqrt{2\gamma P_j}. \tag{20}$$

Following the procedure described in the Appendix, we obtain the third order phase equation

$$\frac{1}{\Omega_j^2}\left[\frac{d^3\Phi_j}{dt^3}+\gamma(2P_j+1)\frac{d^2\Phi_j}{dt^2}\right]+\frac{d\Phi_j}{dt} = \omega_j-\frac{\alpha\eta}{N}\sum_{n=1}^{N}\sin[\vartheta_{jn}+\Phi_j-\Phi_n(t-t_D)] - \frac{\alpha\chi}{2}\sum_{p=j-1,j+1}\sin(\zeta+\Phi_j-\Phi_p). \tag{21}$$

These equations generalize the phase equation (3) by the presence of higher order derivatives of Φ_j. The left hand side of Eq. (21) has a structure similar to the equation derived in Ref. [20] for a multimode single SCL with external feedback. One can also note an analogy between Eq. (21) and the extended Kuramoto model, studied in Refs. [21,22], in which a second derivative of the phase variable was included in order to take into account ''inertial'' effects. The authors of Ref. [21] found, in the limit $N\to\infty$, that inertia ''embarrasses'' the in-phase synchronization. In our case inertial terms proportional to higher order derivatives in Eq. (21) are responsible for the appearance of self-pulsing instabilities at $\eta=\eta_{H1}$ and $\eta=\eta_{H2}$. As already mentioned, the first of these two instabilities leads to the solutions with partially broken in-phase synchrony.

We derive amplitude equations by following the two-time scale perturbation approach proposed in Ref. [23]. To this end, we introduce the two time variables s and τ and their delays by

$$(s,s_D)=\overline{\Omega}(t,t_D), \quad (\tau,\tau_D)=\gamma(\overline{P}+1/2)(t,t_D), \tag{22}$$

where $\overline{\Omega}=\sqrt{2\gamma\overline{P}}$. Coupling parameters and frequencies are rescaled as

$$(K,X,\delta\omega_j,\delta\Omega_j)=\frac{(\alpha\eta,\alpha\chi,\omega_j-\overline{\omega},\Omega_j-\overline{\Omega})}{\gamma(\overline{P}+1/2)},$$

and $\delta\Omega_j=(P_j-\overline{P})/[\overline{\Omega}(\overline{P}+1/2)]$. In the leading order approximation, one obtains

$$x_j=-\mathrm{Im}[z_j(\tau)e^{is}], \quad y_j=\mathrm{Re}[z_j(\tau)e^{is}],$$

$$\Phi_j=\overline{\omega}t+\phi_j(\tau)+\mathrm{Re}[z_j(\tau)e^{is}] \tag{23}$$

In the Appendix, we derive the slow time evolution equations for $\phi_j(\tau)$ and $z_j(\tau)$:

$$\frac{d\phi_j}{d\tau}=\delta\omega_j-\frac{K}{N}\sum_{n=1}^{N}\sin(\phi_{jn})J_0(|z_{jn}|) - \frac{X}{2}\sum_{q=j-1,j+1}\sin(\xi_{jq})J_0(|w_{jq}|), \tag{24}$$

$$\frac{dz_j}{d\tau}=(-1+i\,\delta\Omega_j)z_j+\frac{K}{N}\sum_{n=1}^{N}\cos(\phi_{jn})z_{jn}\frac{J_1(|z_{jn}|)}{|z_{jn}|} + \frac{X}{2}\sum_{q=j-1,j+1}\cos(\xi_{jq})w_{jq}\frac{J_1(|w_{jq}|)}{|w_{jq}|}. \tag{25}$$

In these equations, $J_\nu(x)$ are Bessel functions of the first kind, and

$$\phi_{jn}=\overline{\omega}t_D+\vartheta_{jn}+\phi_j-\phi_n(\tau-\tau_D),$$

$$z_{jn}=z_j-z_n(\tau-\tau_D)\exp(-is_D), \tag{26}$$

$$\xi_{jq}=\zeta+\phi_j-\phi_q, \quad w_{jq}=z_j-z_q. \tag{27}$$

We use the amplitude equations (24) and (25) in order to describe analytically periodic self-pulsing regimes in the array. Specifically, the steady state $z_1=\cdots=z_N=0$ of Eqs. (24) and (25) corresponds to the cw solutions of the original Lang-Kobayashi equations, whereas the states with time independent $|z_j|\neq 0$ correspond to periodic self-pulsing solutions of Eqs. (1) and (2). Although, for the sake of generality, local coupling and dispersion in natural frequencies are included in Eqs. (24) and (25), below we focus on the synchronization of globally coupled oscillators with identical parameters in the absence of local coupling: $X,\delta\Omega_j,\delta\omega_j,\vartheta_{jn}=0$.

A. In-phase periodic solution

An in-phase periodic solution of Eqs. (1) and (2), that bifurcates at $\eta=\eta_{H2}$, is obtained by substituting $\phi_j=\Delta\omega\tau$ and $z_j(\tau)=\rho\exp(i\Delta\Omega\tau)$ with a time independent ρ in Eqs. (24) and (25). The amplitude ρ of the oscillations is then related to the coupling parameter K by the implicit relations

$$K^{-1}=\frac{\tilde{\rho}J_1(\tilde{\rho})}{2\rho^2}\cos\psi,\quad \tilde{\rho}=2\rho\sin(\varphi/2), \tag{28}$$

$$\psi=\overline{\omega}t_D+\Delta\omega\tau_D,\quad \varphi=\overline{\Omega}t_D+\Delta\Omega\tau_D, \tag{29}$$

where the frequency shifts $\Delta\omega$ and $\Delta\Omega$ obey the transcendental equations

$$\Delta\omega=-2\frac{\rho^2J_0(\tilde{\rho})}{\tilde{\rho}J_1(\tilde{\rho})}\tan\psi,\quad \Delta\Omega=\cot\left(\frac{\varphi}{2}\right). \tag{30}$$

Equations (30) for the correction to the relaxation oscillation frequency $\Delta\Omega$ is in fact equivalent to Eq. (18). The value of φ can be controlled by varying the external cavity length on the cm scale. If the delay is moderate, $\tau_D\ll 1$, one can use the approximation $\psi\simeq\overline{\omega}t_D$. Then Eqs. (28) decouple from the equation for $\Delta\omega$ in Eqs. (30). Note that $K\to K_{H2}=2\sec(\psi)/(1-\cos\varphi)$ as $\rho\to 0$, which is consistent with Eq. (17) for $\alpha\gg 1$ and $\chi=0$. The stability of solutions (28)–(30) can be determined by linearizing Eqs. (24) and (25), and applying a discrete Fourier transformation of variables as in Eq. (5). This yields stability conditions for perturbations transverse to the synchronization manifold.

If $\eta_{H2}<\eta_{H1}$, that is, if $\cos\varphi<0$, the in-phase periodic solution is stable in the vicinity of the self-pulsing threshold. However, it can be destabilized by a secondary bifurcation K_ϕ. The condition $K=K_\phi$ defines an $(N-1)$-fold degenerate steady state bifurcation of Eqs. (24) and (25) which corresponds to a secondary bifurcation of the in-phase periodic solutions of Eqs. (1) and (2). This bifurcation leads to a gradual desynchronization of the optical phases ϕ_j. To demonstrate this point, we perturb the in-phase solutions (28)–(30) as $\phi_j=\Delta\omega\tau+\delta\phi_j$ and $z_j=\rho\exp(i\Delta\Omega\tau)+\delta z_j$. In the particular case $\cos\psi=1$, the linearized equations for $\delta\phi_j$ decouple from those for δz_j:

$$\frac{d\,\delta\phi_j}{d\tau}=-KJ_0(\tilde{\rho})\sum_n\ \delta\phi_j-\delta\phi_n(\tau-\tau_D). \tag{31}$$

According to Eq. (31) the secondary instability $K=K_\phi$ takes place when the quantity $J_0(\tilde{\rho})$ changes from positive to negative with increasing ρ.

If $\eta_{H2}>\eta_{H1}$, the cw regime is already unstable at the Hopf bifurcation $K=K_{H2}$, and the in-phase periodic solution emerging from this point is, therefore, also unstable. However, the laser array can be stabilized in the in-phase state through an $(N-1)$-fold degenerate Hopf bifurcation of Eqs. (24) and (25) at $K=K_\theta$. This corresponds to a secondary antiphase Hopf bifurcation of the in-phase self-pulsing solution in the original laser equations. Further increasing K, the laser array again loses its in-phase synchronization at $K=K_\phi>K_\theta$. This situation is illustrated by the bifurcation diagram shown in Fig. 4(a) [27]. In this figure, the branches of stable self-pulsing solutions bifurcating from the in-phase cw state are shown as functions of the coupling strength. It is seen that in-phase and antiphase self-pulsing regimes can coexist in a broad range of coupling strengths. The bifurcation thresholds $K=K_\theta$ and $K=K_\phi$ are shown in Fig. 5 as functions of ωt_D.

The bifurcation diagram shown in Fig. 6 corresponds to a large value of the delay, $\tau_D=1.83$, for which the in-phase Hopf bifurcation always precedes the antiphase Hopf bifurcation. As seen from the figure, the stable in-phase self-pulsing solution emerging at $\eta=\eta_{H2}$ undergoes a secondary Hopf bifurcation to an in-phase synchronized solution with quasiperiodic laser intensities. Since this secondary bifurcation takes place before the desynchronizing bifurcation at $K=K_\phi$, in-phase synchronization is preserved in the quasiperiodic self-pulsing regime. This eventually leads to an in-phase synchronized chaotic regime with increasing η.

B. Antiphase periodic solutions

From the linear stability analysis, we know that the antiphase self-pulsing solutions can destabilize the cw in-phase state only if τ_D is sufficiently small. Otherwise, $\eta_{H2}<\eta_{H1}$, and the in-phase periodic solution emerges first. Let us assume that $\tau_D\ll 1$ and, therefore, neglect the delay τ_D in Eq. (26). Substituting $\phi_j=\Delta\omega\tau$ and $z_j=\rho\exp(i\Delta\Omega\tau+2ijk\pi/N)$ in Eqs. (24) and(25), we obtain the following relation between the amplitude ρ of the antiphase selfpulsing solution with the discrete wave number k and the coupling parameter K:

$$K^{-1}=\frac{\cos(\omega t_D)}{N}\sum_{n=1}^{N}\frac{\rho_{n,k}J_1(\rho_{n,k})}{2\rho^2}, \tag{32}$$

where

$$\rho_{n,k}=2\rho\sin\left(\frac{\overline{\Omega}t_D}{2}-\frac{nk\pi}{N}\right).$$

Letting $\rho\to 0$ in Eq. (32), we obtain $K\to K_{H1}=2/\cos(\omega t_D)$, which is consistent with Eq. (16) for $\chi=0$ and $\alpha\to\infty$. All these solutions have the same scaling near $K=K_{H1}$, namely, $\rho=\sqrt{8\Delta K/3}+O(\Delta K^{3/2})$ with $\Delta K=K/K_{H1}-1$, except the solution corresponding to $k=N/2$ with N even, which scales as

$$\rho=\sqrt{\frac{8\Delta K}{3+\cos(2\overline{\Omega}t_D)}}+O(\Delta K^{3/2}). \tag{33}$$

The self-pulsing antiphase solution with the wave number $k=N/2$ is often observed in numerical simulations when N is even in Eqs. (1) and (2). For this wave number, two clusters form in the array. Within each cluster, individual laser intensities oscillate in phase, while SCL's pertaining to different clusters differ by a phase shift of π in their relaxation oscil-

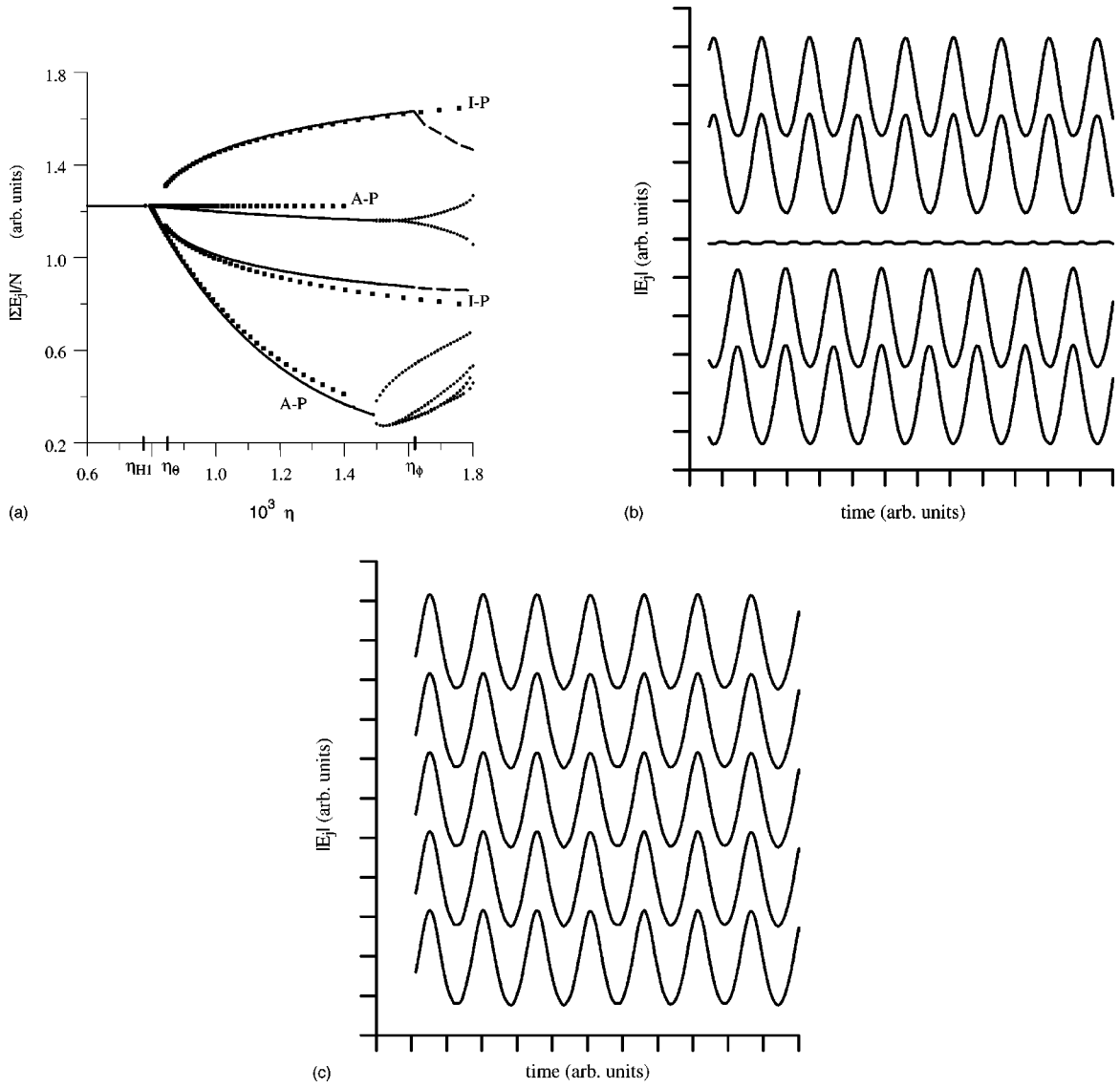

FIG. 4. (a) Branches of self-pulsing solutions bifurcating from the in-phase cw state obtained by simulating numerically Eqs. (1) and (2) with $N=5$, $\mathrm{mod}(\overline{\omega}t_D,2\pi)=0.14$ and $t_D=91.7$, which corresponds to $\overline{\Omega}t_D=5.02$ and $\tau_D=0.18$. The minima and maxima of the total field are plotted as functions of η. Other parameters are the same as in Fig. 2. The secondary bifurcation η_θ (η_ϕ) corresponds to K_θ (K_ϕ) discussed in Sec. V A. Dotted lines are the analytical approximations for the self-pulsing solutions obtained using Eqs. (28)–(30), (34) and (35). (b) Laser intensities for the antiphase self-pulsing branch AP of (a). $\eta=1.12\times10^{-3}$. (c) Intensities for the in-phase self-pulsing branch IP of (a). $\eta=1.12\times10^{-3}$.

lations. The denominator in Eq. (33) indicates that the growth rate of the amplitude of this self-pulsing state with ΔK is maximum for $\cos(2\overline{\Omega}t_D)=-1$. Such a resonance condition, with respect to the frequency $2\overline{\Omega}$, is connected to the fact that the total reflected field oscillates at twice the oscillation frequency of the individual lasers if the laser array is in the $k=N/2$ state. Indeed, let us reconstruct $E_{tot}=\Sigma_{j=1}^{N}E_j$ using Eq. (19) and $\phi_j=\Delta\omega\tau$, z_j zj$=(-1)^j\rho\exp(i\Delta\Omega\tau)$:

$$E_{tot}\propto\cos[\rho\cos(\overline{\Omega}t+\Delta\Omega\tau)]+O(\rho/\alpha)$$
$$\simeq J_0(\rho)-2J_2(\rho)\cos(2\overline{\Omega}t+2\Delta\Omega\tau).$$

With the increase of the coupling strength, a symmetry breaking instability of the $k=N/2$ solution takes place by which the two antiphase clusters acquire different optical phases. In order to demonstrate this phenomenon, we substitute into Eqs. (24) and (25) a perturbed antiphase solution in the form $\phi_j=\Delta\omega\tau+(-1)^j\delta\phi$, $z_j=(-1)^j\rho\exp(i\Delta\Omega\tau)+(-1)^j\delta z$, and derive linearized equations for $\delta\phi$ and δz. In the particular case $\cos(\omega t_D)=1$, the equation for $\delta\phi$ does not depend on δz, and is

$$\frac{d\,\delta\phi}{d\tau}=-KJ_0[2\rho\cos(\overline{\Omega}t_D/2)]\delta\phi.$$

Accordingly, the symmetry breaking bifurcation arises when

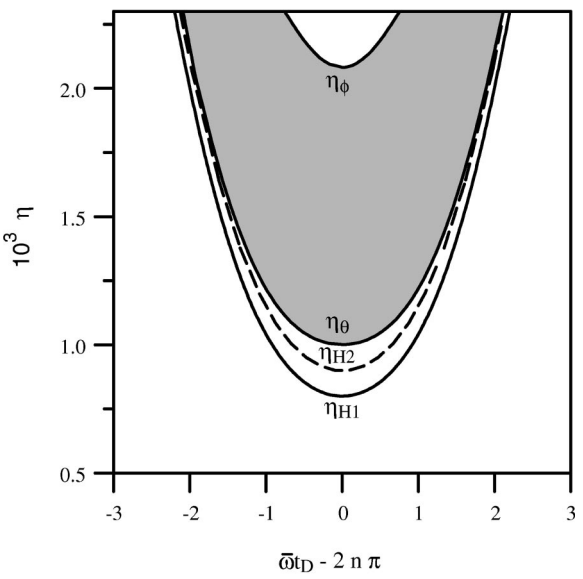

FIG. 5. Bifurcation loci of the in-phase self-pulsing solution labelled IP in Fig. 4(a). The curve η_{H2} corresponds to the Hopf bifurcation from the already unstable cw in-phase solution. The in-phase self-pulsing solution exists above this curve, and is stable in the grey region delimited by the curves η_θ and η_ϕ.

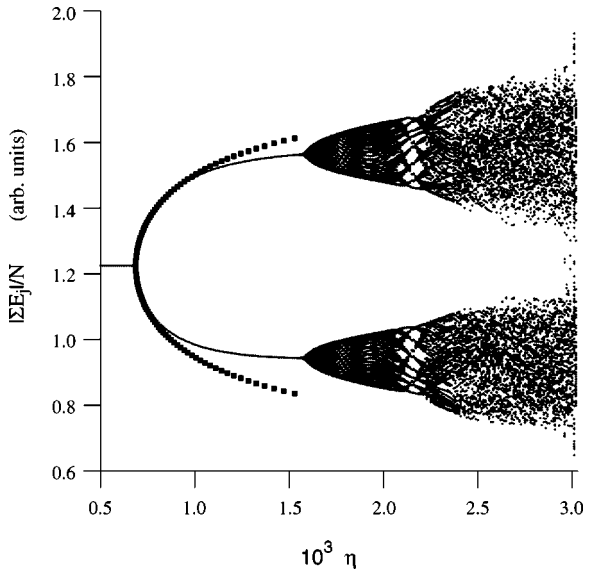

FIG. 6. (a) Numerically calculated bifurcation diagram for Eqs. (1) and (2) with $N=4$, $\mathrm{mod}(\bar{\omega}t_D,2\pi)=0.14$ and $t_D=917$, which corresponds to $\bar{\Omega}t_D=50.2$ and $\tau_D=1.83$. Other parameters are the same as in Fig. 2. The cw in-phase state undergoes the Hopf bifurcation, leading to a stable in-phase self-pulsing solution. With the increase of the coupling strength η, this solution bifurcates into a quasiperiodic in-phase synchronized regime via a secondary Hopf bifurcation. The latter regime bifurcates to a chaotic in-phase synchronized regime as η is further increased. Dotted lines show analytical results obtained using Eqs. (28)–(30).

$J_0[2\rho\cos(\bar{\Omega}t_D/2)]$ becomes negative with increasing ρ. The total field for the solution with the optical phase difference $\delta\phi$ of the antiphase clusters can be written as

$$E_{tot}\propto\cos[\rho\cos(\bar{\Omega}t+\Delta\Omega\tau)+\delta\phi]+O(\rho/\alpha).$$

Note that the trigonometric expression above possess two distinct minima at $\cos(\delta\phi\pm\rho)$. A similar feature is exhibited by the antiphase self-pulsing regime bifurcating at $\eta=1.49$ in Fig. 4(a).

Two antiphase clusters can appear in the array if N is odd, except that one laser does not belong to any cluster. The first order amplitude equations (24) and (25) predict that this laser is in a steady state. Higher order effects lead to corrections in the form of very small amplitude oscillations. This behavior is illustrated in Fig. 4(b), and corresponds to the branch of the solution labeled AP in Fig. 4(a). In Fig. 4(b), two antiphase clusters are formed by lasers 1 and 2 and 4 and 5, whereas laser 3 is almost cw. A self-pulsing solution with two antiphase clusters and a single cw laser can be described analytically with the help of Eqs. (24) and (25). Looking for a solution of the forms $z_1=0$, $z_{j>1}=(-1)^j\rho\exp(i\Delta\Omega\tau)$, $\phi_{j>1}=\Delta\omega\tau$, and $\phi_1=\Delta\omega\tau-\delta\phi$, and using the self-consistency condition $d\phi_1/d\tau=d\phi_{j>1}/d\tau$, we obtain a transcendental equation for the optical phase lag $\delta\phi$:

$$(N-2)\cos(\delta\phi)-N\cot(\omega t_D)\sin(\delta\phi)=\frac{(N-1)[J_0(\rho_+)+J_0(\rho_-)]-2}{2J_0(\rho)},\qquad(34)$$

where $\rho_+=2\rho\cos(\bar{\Omega}t_D/2)$ and $\rho_-=2\rho\sin(\bar{\Omega}t_D/2)$. The amplitude ρ and the coupling parameter K are related by

$$K^{-1}=\cos(\omega t_D+\delta\phi)\frac{J_1(\rho)}{N\rho}+\frac{N-1}{N}\cos(\omega t_D)\frac{\rho_-J_1(\rho_-)+\rho_+J_1(\rho_+)}{4\rho^2}.\qquad(35)$$

Due to the permutation symmetry of the problem with $\chi=0$, the laser indices can be rearranged such that the $(N-1)/2$ first lasers belong to the first cluster and the $(N-1)/2$ last lasers form the second cluster. The cw laser is thus at the center, and can be viewed as a transition point between the two clusters where a sudden relaxation phase shift of π takes place. Numerical simulations with nonzero but small χ and boundary conditions $E_0=E_{N+1}=0$ lead to such a situation. This state of synchronization can therefore be viewed as a discrete analog of a domain wall.

VI. CONCLUSION

We have studied the synchronization properties of a SCL array subjected to a delayed global coupling through optical feedback. If the lasers are identical and the coupling strength is below the self-pulsing threshold, the array dynamics can be modeled with Kuramoto phase equations (3) that include a time delay. Depending on the optical dephasing of the feedback field, the coupling induces either in-phase or antiphase cw synchronization. Increasing the time delay, the stability domains expand for the in-phase cw states, whereas

they shrink and tend to disappear for the antiphase cw states [compare Figs. 3(a) and 3(b)]. In the more realistic situation where there is a distribution of the SCL's optical frequencies, the coupling strength must exceed some critical value η_c in order to establish synchronization. An estimation of η_c, given by Eq. (13), can be obtained from the Kuramoto model [Eq. (3)] in the limit of an infinitely large array [3,4]. We note, however, that a more complete description of the laser synchronization properties can be expected from the extended model [Eq. (21)], because it takes into account weakly damped relaxation oscillations. These oscillations are typical of solid state and semiconductor lasers. Though damped, they could degrade the synchronization properties of the array. Recently, it was shown that a second order derivative term included in the Kuramoto phase equations can increase the in-phase synchronization threshold [21].

As the coupling strength exceeds the Hopf bifurcation threshold, the laser intensities become time periodic. They exhibit either in-phase or antiphase pulsations, with a frequency close to the relaxation oscillations frequency Ω of the solitary SCL. Antiphase dynamics is a common feature typical of many other systems consisting of globally coupled identical elements [24–26]. A Hopf bifurcation, leading to antiphase dynamics, exists even in the absence of time delay. Conversely, in-phase self-pulsing instability can appear only if $\Omega t_D = O(1)$. For moderate delays, i.e., $\Omega t_D = O(1)$, which of the two self-pulsing bifurcations destabilizes the cw in-phase state depends on the relaxation dephasing between the emitted and reinjected fields. In this case we found that even if the antiphase Hopf bifurcation takes place first, the in-phase self-pulsing solution can become stable with the increase of the coupling strength, illustrated by Fig. 4(a). On the other hand, for large delays, verifying $t_D \gtrsim \pi\gamma^{-1}(2\overline{P}+1)^{-1}$, the in-phase bifurcation always precedes the antiphase one, thus preserving in-phase synchrony in the self-pulsing regime.

Above the self-pulsing threshold, the phase equations (3) are no longer valid. Therefore, in order to describe the self-pulsing dynamics, we use an extended version of the Kuramoto model with higher order derivative terms [Eq. (21)]. Using a perturbation method, we reduced Eqs. (21) to the amplitude equations (24) and (25). This allowed us to describe analytically various self-pulsing solutions emerging from the Hopf bifurcations, and discuss their stability. In particular, we have studied secondary antiphase bifurcations of the in-phase self-pulsing solution. For moderate delays, $\Omega t_D = O(1)$, these bifurcations can destroy the synchrony of the in-phase self-pulsing regime, and, hence, decrease the amplitude of the total field $\Sigma_{j=1}^{N} E_j$. However, if $t_D \sim \gamma^{-1}$, they are bypassed by another secondary bifurcation that leads to in-phase synchronized output with quasiperiodic laser intensities. Numerically, in-phase synchrony is then seen to persist even in the chaotic regimes.

Finally we have described a particular antiphase state featuring extinction of the sustained relaxation oscillations of a single laser. The existence of such stable regime was verified by means of numerical simulations of the original laser equations (1) and (2). If a weak local coupling is added to the system, the cw laser becomes a discrete analog of a domain wall.

Thus we can conclude that the effect of time delay is essentially to increase the complexity of the array dynamics by producing new branches of in-phase cw, periodic, quasiperiodic, or chaotic solutions. The symmetry of the global coupling imposes that these solutions lie within the in-phase synchronization manifold, where all the elements of the array behave identically. For large delays, the bifurcations by which in-phase solutions are created precede antiphase instabilities. In this way, the phase trajectory may be kept in the in-phase synchronization manifold.

ACKNOWLEDGMENTS

This research was supported by the Fonds National de la Recherche Scientifique, the Inter-University Attraction Pole program of the Belgian government, and an INTAS grant.

APPENDIX: DERIVATION OF THE SOLVABILITY CONDITION

Substituting Eqs. (19) and (20) into Eqs. (1) and (2) yields

$$\frac{dx_j}{dt} = -\gamma(1+2P_j)x_j - \Omega_j y_j + O(\sqrt{\gamma}/\alpha), \tag{A1}$$

$$\frac{dy_j}{dt} = \Omega_j x_j + \frac{\alpha\eta}{N}\sum_{n=1}^{N} \sin[\vartheta_{jn} + \Phi_j - \Phi_n(t-t_D)] + \frac{\alpha\chi}{2}\sum_{p=j-1,j+1} \sin(\zeta + \Phi_j - \Phi_p) + O(\sqrt{\gamma}/\alpha, \eta, \chi, \alpha\eta\delta P_j, \alpha\chi\delta P_j), \tag{A2}$$

$$\frac{d\Phi_j}{dt} = \omega_j + \Omega_j x_j + O(\eta, \chi). \tag{A3}$$

where $\delta P_j = P_j/\overline{P} - 1$. In these equations, we keep terms of order $\alpha\eta$, $\alpha\chi$, and γ, because they are of the same order at the bifurcation points [Eqs. (16) and (17)]. Differentiating Eq. (A3) twice with respect to time, and using Eqs. (A1) and (A2), one obtains Eqs. (21).

Next we introduce the two time scales in Eq. (22) and expand the dependent variables in Eqs. (A1)–(A3) as

$$\begin{aligned} x_j &= x_j^{(0)}(s,\tau) + \sqrt{\gamma}x_j^{(1)}(s,\tau) + \cdots, \\ y_j &= y_j^{(0)}(s,\tau) + \sqrt{\gamma}y_j^{(1)}(s,\tau) + \cdots, \\ \Phi_j &= \overline{\omega}t + \Phi_j^{(0)}(s,\tau) + \sqrt{\gamma}\Phi_j^{(1)}(s,\tau) + \cdots. \end{aligned} \tag{A4}$$

Collecting $O(\gamma^0)$ terms, we obtain

$$\left(\frac{\partial}{\partial s} - \mathcal{L}\right)\begin{pmatrix} x_j^{(0)} \\ y_j^{(0)} \\ F_j^{(0)} \end{pmatrix} = 0, \quad \mathcal{L} = \begin{pmatrix} 0 & -1 & 0 \\ 1 & 0 & 0 \\ 1 & 0 & 0 \end{pmatrix}. \tag{A5}$$

This equation has the solutions

$$x_j^{(0)} = -\mathrm{Im}[z_j(\tau)e^{is}], \quad y_j^{(0)} = \mathrm{Re}[z_j(\tau)e^{is}], \qquad \text{(A6)}$$

$$\Phi_j^{(0)} = \phi_j(\tau) + \mathrm{Re}[z_j(\tau)e^{is}].$$

Next, equating the terms of order $\gamma^{1/2}$, we obtain

$$\left(\frac{\partial}{\partial s} - \mathcal{L}\right)\begin{pmatrix} x_j^{(1)} \\ y_j^{(1)} \\ F_j^{(1)} \end{pmatrix} = \frac{\overline{P}+1/2}{\sqrt{2\overline{P}}}\vec{\mathcal{B}}. \qquad \text{(A7)}$$

The quantity $\vec{B}$ on the right-hand side of Eq. (A7) is computed using the following properties of Bessel functions:

$$\sin[\overline{\omega}t_D + \vartheta_{jn} + \Phi_j^{(0)} - \Phi_n^{(0)}(s-s_D)]$$
$$= J_0(|z_{jn}|)\sin\phi_{jn} + \frac{J_1(|z_{jn}|)}{|z_{jn}|}(z_{jn}e^{is} + \text{c.c.})$$
$$\times \cos\phi_{jn} + \text{h.h.},$$

and

$$\sin(\zeta + \Phi_j^{(0)} - \Phi_q^{(0)})$$
$$= J_0(|w_{jq}|)\sin\xi_{jq} + \frac{J_1(|w_{jq}|)}{|w_{jq}|}(w_{jq}e^{is} + \text{c.c.})$$
$$\times \cos\xi_{jq} + \text{h.h.},$$

where c.c. and h.h. mean ''complex conjugate'' and ''higher harmonics,'' respectively. This yields

$$\vec{\mathcal{B}} = -\frac{\partial}{\partial\tau}\begin{pmatrix} x_j^{(0)} \\ y_j^{(0)} \\ \Phi_j^{(0)} \end{pmatrix} + \begin{pmatrix} -2x_j^{(0)} - \delta\Omega_j y_j^{(0)} \\ \delta\Omega_j x_j^{(0)} \\ \delta\omega_j \end{pmatrix}$$
$$+ \begin{pmatrix} 0 \\ 1 \\ 0 \end{pmatrix}\left\{\frac{K}{N}\sum_n \left[\sin\phi_{jn}J_0(|z_{jn}|)\right.\right.$$
$$\left.\left. + \cos\phi_{jn}\frac{J_1(|z_{jn}|)}{|z_{jn}|}(z_{jn}e^{is} + \text{c.c.})\right]\right.$$
$$\left. + \frac{X}{2}\sum_{q=j-1,j+1}\left[\sin\xi_{jq}J_0(|w_{jq}|)\right.\right.$$
$$\left.\left. + \cos\xi_{jq}\frac{J_1(|w_{jq}|)}{|w_{jq}|}(w_{jq}e^{is} + \text{c.c.})\right]\right\} + \text{h.h.}$$

The existence of nontrivial solutions of Eq. (A7) implies the orthogonality conditions or solvability conditions

$$\int_0^{2\pi}\vec{v}_0\cdot\vec{\mathcal{B}}ds = 0, \quad \int_0^{2\pi}\vec{v}_\pm\cdot\vec{\mathcal{B}}e^{\pm is}ds = 0,$$

where $\vec{v}_0 = (0,1,-1)$ and $\vec{v}_\pm = (\mp i,1,0)$ are the left eigenvectors of $\mathcal{L}$ associated with the eigenvalues 0 and $\pm i$, respectively. These solvability conditions lead to Eqs. (24) and (25).

The error in Eqs. (24) and (25), related to the assumption $\alpha \gg 1$, can be estimated near the Hopf bifurcation points. To this end, we introduce a small parameter ε by

$$K = K_H + \varepsilon^2 K_2,$$

and seek periodic solutions of the forms

$$f_j = \mathrm{Re}(\varepsilon f_{j,1}e^{is} + \cdots), \quad f_j = x_j, y_j, \Phi_j - \overline{\omega}t.$$

This produces a set of linear differential equations at each order in ε. At third order, the solvability condition yields the corrected version of Eq. (25) in the vicinity of the bifurcation point:

$$\frac{dz_j}{d\tau} = -\frac{i\sqrt{2\overline{P}}}{12\alpha^2\sqrt{\gamma}(2\overline{P}+1)}z_j|z_j|^2$$
$$+ \frac{K_H\cos\psi}{16N}\sum_n z_{jn}\left(8\frac{K-K_H}{K_H} - |z_{jn}|^2\right) + O(\alpha^{-1}).$$

The principal correction to Eq. (25), close to the bifurcation point, is thus $O(\alpha^{-2}\gamma^{-1/2})$. Since it is imaginary, it only affects the relaxation frequency and not the amplitude of the oscillations. The next corrections are only $O(\alpha^{-1})$, which explains the good agreement between numerical and theoretical curves in Figs. 4(a) and 6.

[1] Y. Kuramoto, *Chemical Oscillations, Waves, and Turbulence* (Springer-Verlag, Berlin, 1984).

[2] S.H. Strogatz, Physica D **143**, 1 (2000).

[3] M.K.S. Yeung and S.H. Strogatz, Phys. Rev. Lett. **82**, 648 (1999).

[4] M.Y. Choi, H.J. Kim, D. Kim, and H. Hong, Phys. Rev. E **61**, 371 (2000).

[5] S. Kim, S.H. Park, and C.S. Ryu, Phys. Rev. Lett. **79**, 2911 (1997).

[6] D.V. Ramana Reddy, A. Sen, and G.L. Johnston, Phys. Rev. Lett. **80**, 5109 (1998).

[7] G. Kozyreff, A.G. Vladimirov, and P. Mandel, Phys. Rev. Lett. **85**, 3809 (2000).

[8] R.-D. Li and T. Erneux, Opt. Commun. **99**, 196 (1993).

[9] J. Garcia-Ojalvo, J. Casademont, C.R. Mirasso, M.C. Torrent, and J.M. Sancho, Int. J. Bifurcation Chaos Appl. Sci. Eng. **9**, 2225 (2000).

[10] S.Y. Kourtchatov, V.V. Likhanskii, A.P. Napartovich, F.T. Arecchi, and A. Lapucci, Phys. Rev. A **52**, 4089 (1995).

[11] J. Yaeli, W. Streifer, D.R. Scifres, and P.S. Cross, Appl. Phys. Lett. **47**, 89 (1985); C. Chang-Hasnain, D.F. Welch, D.R. Scifres, J.R. Whinnery, A. Dienes, and R.D. Burnham, *ibid.* **49**, 614 (1986); C.J. Chang-Hasnain, J. Berger, D.R. Scifres, W. Streifer, J.R. Whinnery, and A. Dienes, *ibid.* **50**, 1465 (1987); J.R. Leger, *ibid.* **55**, 334 (1989); F.X. D'Amato, E.T. Siebert, and C. Roychoudhuri, *ibid.* **55**, 816 (1989); J.R. Leger, M.L.

Scott, and W.B. Veldkamp, *ibid.* **52**, 1771 (1988); V.P. Kandidov and A.V. Kondratev, Laser Phys. **10**, 1089 (2000); A.F. Glova, *ibid.* **10**, 975 (2000).
[12] S. Wolff and H. Fouckhardt, Opt. Express **7**, 222 (2000).
[13] Motoichi Ohtsu, *Highly Coherent Semiconductor Lasers* (Artech House, Bristol, 1992), pp. 124–140.
[14] D. Lenstra, B.H. Verbeek, and A.J. den Boef, IEEE J. Quantum Electron. **QE-21**, 674 (1985); Y. Cho and T. Umeda, Opt. Commun. **59**, 131 (1986); J. Mork, B. Tromborg, and J. Mark, IEEE J. Quantum Electron. **28**, 93 (1992); G.H.M. van Tartwijk and D. Lenstra, Quantum Semiclassic. Opt. **7**, 87 (1995); D. Pieroux, T. Erneux, and P. Mandel, Phys. Rev. A **54**, 3409 (1994); P. Saboureau, J.-P. Foing, and P. Schanne, IEEE J. Quantum Electron. **33**, 1582 (1997).
[15] S.S. Wang and H.G. Winful, Appl. Phys. Lett. **52**, 1774 (1988); H.G. Winful and S.S. Wang, *ibid.* **52**, 1894 (1988).
[16] M. Silber, L. Fabiny, and K. Wiesenfeld, J. Opt. Soc. Am. B **10**, 1121 (1993).
[17] S. Nichols and K. Wiesenfeld, Phys. Rev. A **45**, 8430 (1992).
[18] S.H. Strogatz and R.E. Mirollo, Phys. Rev. E **47**, 220 (1993).
[19] A.G. Vladimirov, E.A. Viktorov, and P. Mandel, Phys. Rev. E **60**, 1616 (1999).
[20] T.W. Carr, D. Pieroux, and P. Mandel, Phys. Rev. A **63**, 033817 (2001).
[21] J.A. Acebrón and R. Spigler, Phys. Rev. Lett. **81**, 2229 (2000); J.A. Acebrón, L.L. Bonilla, and R. Spigler, Phys. Rev. E **62**, 3437 (2000).
[22] L.L. Bonilla, Phys. Rev. E **62**, 4862 (2000).
[23] P.M. Alsing, V. Kovanis, A. Gavrielides, and T. Erneux, Phys. Rev. A **53**, 4429 (1996).
[24] P. Hadley and M.R. Beasley, Appl. Phys. Lett. **50**, 621 (1987); K. Wiesenfeld and P. Hadley, Phys. Rev. Lett. **62**, 1335 (1989); K. Yoshimoto, K. Yoshikawa, Y. Mori, and I. Hanazaki, Chem. Phys. Lett. **189**, 18 (1992); W.J. Freeman and C.A. Skarda, Brain Res. Rev. **10**, 47 (1985).
[25] K. Wiesenfeld, C. Bracikowski, G. James, and R. Roy, Phys. Rev. Lett. **65**, 1749 (1990); C. Bracikowski and R. Roy, Chaos **1**, 49 (1991); K. Otsuka, Phys. Rev. Lett. **67**, 1090 (1991); S. Bielawski, D. Derozier, and P. Glorieux, Phys. Rev. A **46**, 1692 (1992); J.-Y. Wang and P. Mandel, *ibid.* **48**, 671 (1993); J.-Y. Wang, P. Mandel, and T. Erneux, Quantum Semiclassic. Opt. **7**, 169 (1994); J.-Y. Wang and P. Mandel, Phys. Rev. A **52**, 1474 (1995).
[26] P. Mandel, *Theoretical Problems in Cavity Nonlinear Optics* (Cambridge University Press, Cambridge, 1997).
[27] Numerical simulations were performed with ''Dynamics Solver'' by J.M. Aguirregabiria, available at http://tp.lc.ehu.es/jma.html